JOURNAL OF MATERIALS SCIENCE 24 (1989) 3449–3455

Combustion synthesis of TiNi intermetallic compounds

Part 1 *Determination of heat of fusion of TiNi and heat capacity of liquid TiNi*

H. C. YI*, J. J. MOORE†
*Department of Chemical and Materials Engineering, University of Auckland, Auckland, New Zealand
†Department of Metallurgical and Materials Engineering, Colorado School of Mines, Golden, Colorado 80401, USA

The synthesis of the TiNi intermetallic compound using the thermal explosion mode of the combustion synthesis technique has been used to determine the heat of fusion, ΔH_m (7.77 kcal mol^{-1}), of the TiNi intermetallic and the heat capacity, C_{p_l} (17.96 cal mol^{-1} K^{-1}), of the liquid-phase TiNi. The effect of heating rate and degree of dilution of the Ti + Ni powder compact reactants with previously synthesized TiNi on the ignition, T_{ig}, and combustion, T_c, temperatures in an argon atmosphere have been determined. It was found that T_c was dependent on heating rate and dilution with TiNi, whereas T_{ig} remained unchanged with respect to these two process variables.

1. Introduction

Combustion synthesis or self-propagating high temperature synthesis (SHS) is a new method used to synthesize refractory materials such as borides, nitrides, carbides, ceramic composites and intermetallic compounds [1–4]. SHS can be effected using one of two synthesizing modes, i.e. propagating or combustion mode and bulk or thermal explosion mode. In the combustion mode, the reactants, in the form of compacted powder pellets, are ignited by a high-temperature source. Once ignited, the combustion wave propagates through the powder compact leaving the reacted product behind. The thermal explosion mode involves heating the whole pellet in a furnace at a constant heating rate until it reaches the ignition temperature, T_{ig}, which intitiates the reaction as shown in Fig. 1. Because the reaction is exothermic, a maximum temperature, the combustion temperature (T_c), is attained towards the end of the reaction. It has been found that the products from the two modes are exactly the same [5]. The combustion mode is normally used to synthesize refractory materials, whereas thermal explosion is more often used to synthesize intermetallic or metallic alloys which exhibit relatively lower exothermic characteristics.

SHS-produced materials have been reported to have various advantages with respect to energy and time saving. Both the combustion and the thermal explosion modes are completed in a few seconds, although the total time to complete the thermal explosion technique, because heating in a furnace is required, may take a few minutes. This is compared with hours or days used in the conventional reaction sintering processes. Owing to the extremely high combustion temperatures that can be reached, the products are often of high purity, because any lower boiling point contaminants present at such high temperatures, will vaporize. Also, due to the rapid cooling associated with these two modes of synthesis the potential for non-equilibrium, metastable products is possible.

Numerous intermetallic compounds have been synthesized using the SHS method [6, 7]. Recently, near equiatomic TiNi has received some attention because of its unique shape-memory properties. Fig. 2 is the phase diagram of the Ti–Ni alloy system which indicates a melting point for the TiNi alloy of 1513 K. Conventionally, the alloy is produced by a vacuum-induction melting method [8, 9]. Recently, Russian researchers have used the combustion mode to synthesize the TiNi shape-memory alloy (SMA) [10–13]. They claimed that pre-heating was needed because of the relatively low exothermic character of the reactions between titanium and nickel. They also found that the combustion temperature was around the melting point of the alloy and stoichiometry of the final product depended on various processing factors, such as particle size of the reactants and the density of the pellet [13].

In the current investigation, the thermal explosion mode has been used to synthesize successfully the TiNi intermetallic compound. The combustion temperature was found to be much higher than the melting point of the alloy so that a cast alloy was obtained. Both the heat capacity of the liquid-phase TiNi and the heat of fusion of the TiNi have been estimated based on thermodynamic calculations. These data are not available from existing thermodynamic literature.

0022–2461/89 $03.00 + .12 © 1989 Chapman and Hall Ltd.

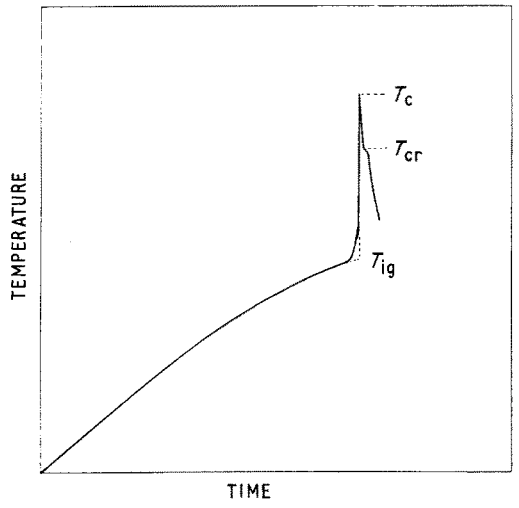

Figure 1 Typical exothermic peak in the combustion of Ti + Ni using the thermal explosion mode.

2. Thermodynamic considerations

Consider the reaction between nickel and titanium to produce the compound TiNi

$$\text{Ti} + \text{Ni} = \text{TiNi} \quad (1)$$

Suppose the reaction occurs at the ignition temperature, T_{ig} (as shown in Fig. 1), the heat liberated during the reaction will be

$$\Delta H^0 = \Delta H_f^0(T_{ig}) + \int_{T_{ig}}^{T_c} C_p(p)\, dT \quad (2)$$

where $\Delta H_f^0(T_{ig})$ is the enthalpy of formation of the compound, TiNi, at temperature T_{ig}, $C_p(p)$ is the heat capacity of the product and T_c is the maximum or combustion temperature attained by the product. Because Reaction 1 is highly exothermic and the reaction time is very short (< 0.5 sec according to the current experimental data) it is reasonable to assume that the reaction occurs adiabatically, i.e. $\Delta H^0 = 0$. Hence Equation 2 becomes

$$-\Delta H_f^0(T_{ig}) = \int_{T_{ig}}^{T_c} C_p(p)\, dT \quad (3)$$

In the current investigation, it has been found that the combustion temperature (T_c) is higher than the melting point (T_m) of the product, so that Equation 3 should be corrected to

$$-\Delta H_f^0(T_{ig}) = \int_{T_{ig}}^{T_m} C_{p_s}(p)\, dT + \Delta H_m + \int_{T_m}^{T_c} C_{p_l}(p)\, dT \quad (4)$$

where ΔH_m is the heat of fusion of the TiNi alloy, $C_{p_s}(p)$ and $c_{p_l}(p)$ are its heat capacities in the solid and liquid phase, respectively. A schematic representation of this process is shown in Fig. 3 in which the thermodynamic data are taken from [14] for $T < T_m$.

On the other hand, $\Delta H_f^0(T_{ig})$ can be calculated from

$$-\Delta H_f^0(T_{ig}) = \Delta H_{f(298)}^0 + \int_{298}^{T_{ig}} \Delta C_p\, dT \quad (5)$$

where $\Delta H_{f(298)}^0$ is the heat of formation of the compound, TiNi, at 298 K and $\Delta C_p = C_p(\text{TiNi}) - [C_p(\text{Ti}) + C_p(\text{Ni})]$ is the change of heat capacity for the reaction. Both of these terms can be obtained from thermodynamic data books [14].

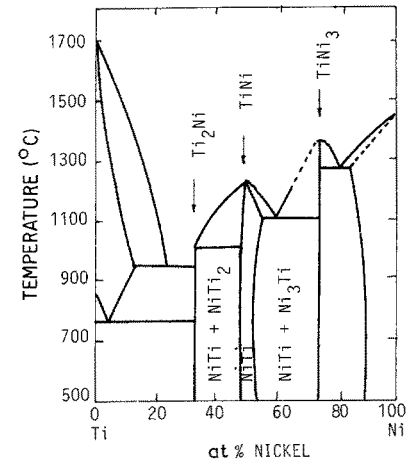

Figure 2 Phase diagram of TiNi alloy after [15].

3. Experimental methods

The powders used in the present investigation were irregularly shaped, -325 mesh ($< 44\,\mu m$) titanium powder and a much coarser, spherically shaped nickel powder, as shown in Fig. 4. Table I gives the sieve

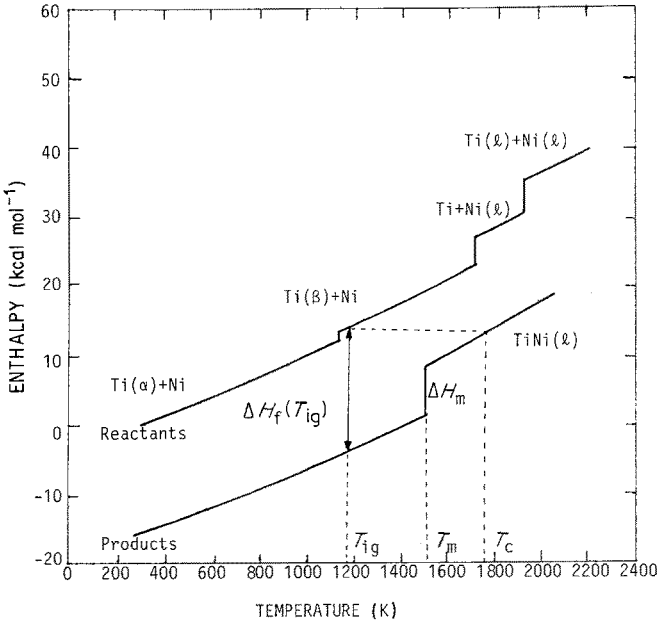

Figure 3 Enthalpy–temperature curves of reactants (Ti + Ni) and product (TiNi) curve: the $T < T_m$ portion has been calculated from [14]. $T > T_m$ has been calculated from the present investigation.

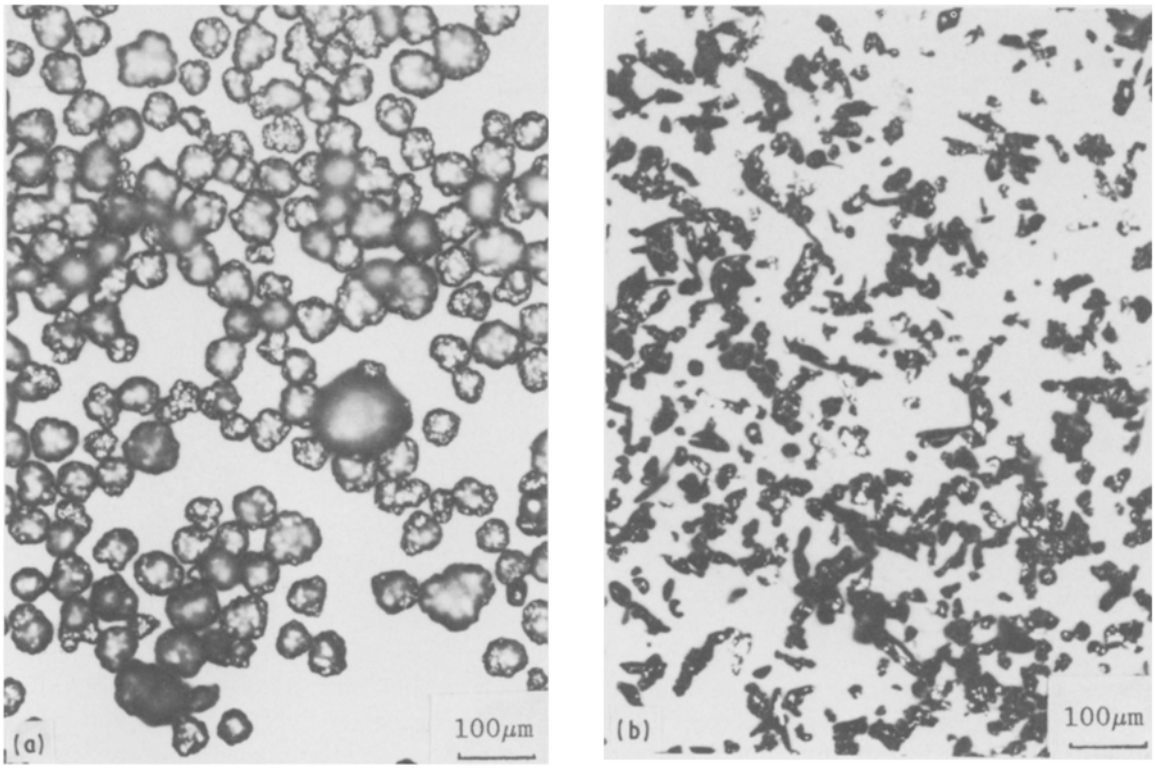

Figure 4 Optical photomicrographs of (a) Ni and (b) Ti powders.

analysis of the nickel powder. The powders were blended at equiatomic stoichiometry and tumbled in a cylindrical container for 5 to 10 min using a mechanical shaker. The pressed pellets were formed in a cylindrical, tool steel die using two plungers. The pressure used was sufficient to give a green density of 67 ± 2% theoretical. The pellets were 7.94 mm diameter and each weighed 1.5 g. A hole of diameter 0.7 mm was drilled at one end of each sample to accommodate the Pt–Pt 13% Rh thermocouple with a diameter of 0.205 mm. The temperature–time relationships (Fig. 1) were recorded during the furnace heating of each sample using a strip chart recorder, from which the heating rate was estimated. As the titanium is very easily oxidized the shorter the heating time the better. The furnace was set at different temperatures between 873 and 1573 K, which allowed variation in the heating rates.

This latter method was used to obtain high heating rates ($> 300\,K\,min^{-1}$), while the lower heating rates ($< 20\,K\,min^{-1}$) were obtained using an EMC programmable controller (EMC Electronics Ltd, Auckland, New Zealand). Previously reacted TiNi product was ground into powder ($< 120\,\mu m$). This was used as a diluent in the titanium and nickel powder mixture in order to investigate the effect of dilution on the combustion synthesis process.

TABLE I Sieve analysis results of nickel powder

Particle size (μm)	Weight per cent
< 44	0.6
45–63	11.5
63–90	25.8
90–125	40.5
125–150	21.6

The microstructure was examined using optical microscopy. The samples were etched in a mixture of 5% HNO_3, 10% HF in water.

4. Results

Fig. 1 shows a typical temperature–time curve for Reaction 1. As the pellet is rapidly heated, Reaction 1 is initiated at the ignition temperature, T_{ig}. The temperature of the pellet increases rapidly within a very short time owing to the adiabatic exothermic reaction. The maximum temperature, T_c, is the combustion temperature which can be assumed to be an adiabatic temperature, T_{ad}. As $T_c > T_m$, a liquid phase was obtained. Under these synthesis conditions, the product is rapidly cooled from T_c until the freezing point is reached at which temperature, T_{cr}, crystallisation of TiNi is initiated. This results in a slight arrest in the temperature–time curve on account of the latent heat of fusion and the intermetallic subsequently cools to the furnace temperature.

Fig. 5 shows the effect of heating rate on the T_{ig} and T_c. As can be seen, when the heating rate was higher than approximately $500\,K\,min^{-1}$, (corresponding to a furnace temperature of 1273 K), T_{ig} remained unchanged at 1183 K. This indicates that the heat needed to generate Reaction 1 is a constant value. At lower heating rates, T_{ig} increased slightly. This is believed to be caused by titanium dioxide formation [15]. Conversely, the combustion temperature was seen to increase initially as the heating rate was increased and eventually levelled out at 1773 K. This resulted in the products being in a liquid state. This combustion temperature determination is approximately 250 K higher than that determined by Itin *et al.* [10–13] who used the combustion mode.

In order to know whether the T_{ig} and T_c values

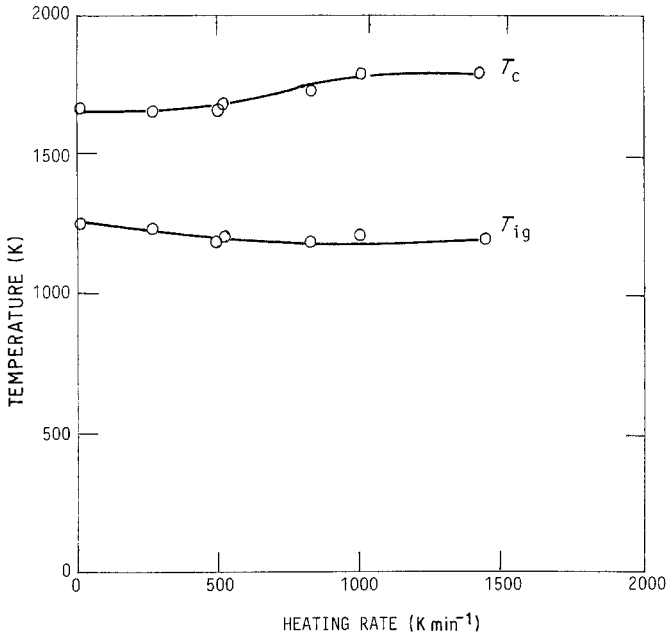

Figure 5 Effect of heating rate on the combustion (T_c) and ignition (T_{ig}) temperatures when combustion was conducted in argon.

determined above were the intrinsic values for Reaction 1, the effect of particle size on the combustion synthesis reaction was investigated. The results are shown in Fig. 6. It can be seen that T_c remained constant regardless of the nickel particle size, whereas T_{ig} increased slightly with decrease in nickel particle size, indicating that the heat dispersion was affected only slightly by nickel particle size.

Fig. 7 shows the effect of dilution with reacted TiNi product on Reaction 1. The combustion temperature remained constant at lower levels of dilution (i.e. up to 12%), but decreased sharply with dilutions greater than 12% of the charge weight.

At dilutions of more than 35% no reaction occurred. It should be noted that in each case the combustion temperature was higher than the melting point of the TiNi intermetallic providing the amount of dilution was less than 35%. Therefore, a cast alloy can always be obtained provided Reaction 1 is initiated.

It can be seen from Fig. 7 that the ignition temperature is a constant value, indicating that the heat needed to generate Reaction 1 is a constant value. Therefore $T_{ig} = 1183\,K$ is an intrinsic value for the titanium and nickel synthesis reaction.

Fig. 8 is a typical photomicrograph of the reacted sample. The product is mainly TiNi with a small amount of Ti_2Ni. This is in accordance with the phase diagram (Fig. 2). Similar results were obtained for the reactions incorporating the TiNi diluent, as shown in Fig. 9. However, increased porosity was evident in these products. Comparing the microstructural features between the non-diluted and diluted reactions, it appeared that the Ti_2Ni was present in a branch-like morphology and more evenly distributed in the non-diluted reacted sample than in the reaction where dilution with TiNi was used. Fig. 10 is a photomicrograph of an area exhibiting a high degree of segregation of Ti_2Ni for a 30% dilution-reacted sample. However, more detailed work needs to be conducted with respect to microstructural features and characterization of these products.

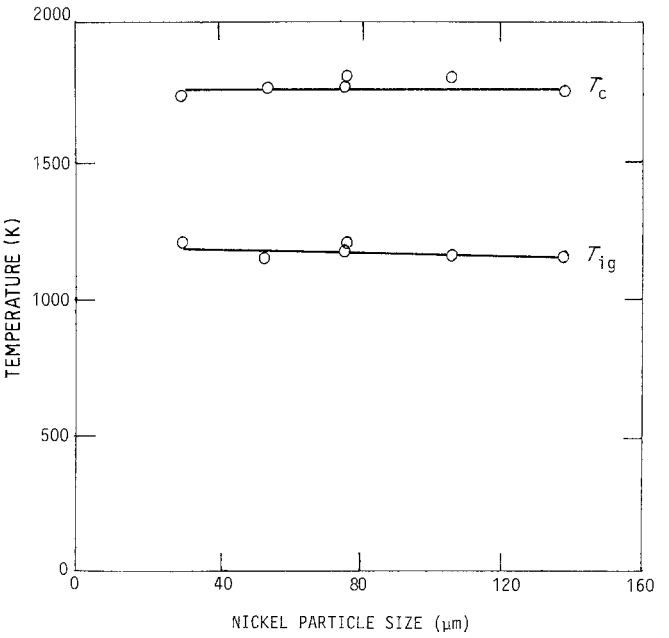

Figure 6 Effect of mean nickel particle size on the combustion (T_c) and ignition (T_{ig}) temperatures.

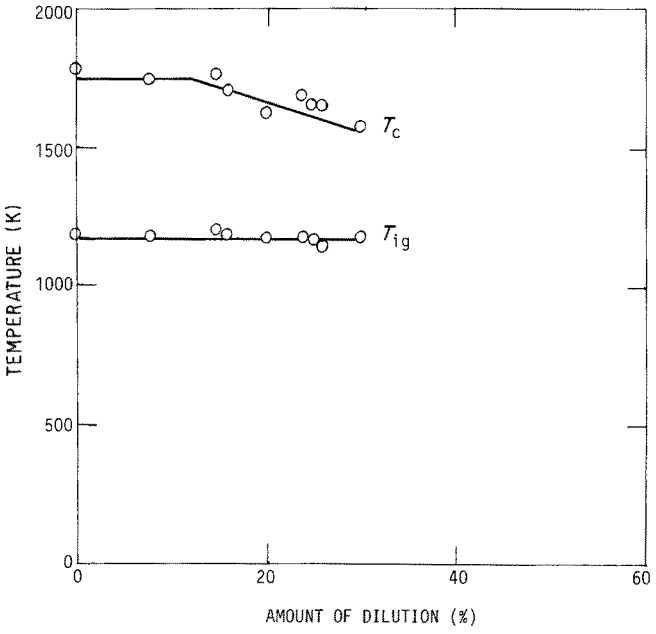

Figure 7 Combustion and ignition temperatures plotted against amount of diluent.

5. Discussion

Using the thermal explosion mode, the whole pellet is heated by an ambient heating source. This is compared with the combustion mode in which the pellet is ignited at one end. In this latter case, heat flow from the reaction zone of the pellet to its surroundings is unavoidable. If this heat flow is too large, the combustion may be quenched. If this heat flow occurs to any extent, the combustion is then non-adiabatic. This perhaps is the reason why the combustion temperature obtained by the combustion mode of synthesis was dependent on various process factors (e.g. diameter and density of the pellets) [10–13], than the thermal explosion mode. This was confirmed by the combustion of Ni-Al by Maslov *et al.* [16] who found that the combustion would not be adiabatic unless the diameter of the pellet was sufficiently large. From this reasoning, it may be argued that the combustion temperature determined by Itin *et al.* [10–13], which was 260 K lower than the present work, was the result of a non-adiabatic combustion process. Therefore, it may be stated that Reaction 1 is a highly exothermic reaction rather than slightly exothermic reaction as proposed by Itin *et al.* [10–13].

In a study of Ni-Al using the thermal explosion mode, Philpot *et al.* [17] found that the heating rate and particle size of the reactants had a great influence on the combustion reaction. The combustion

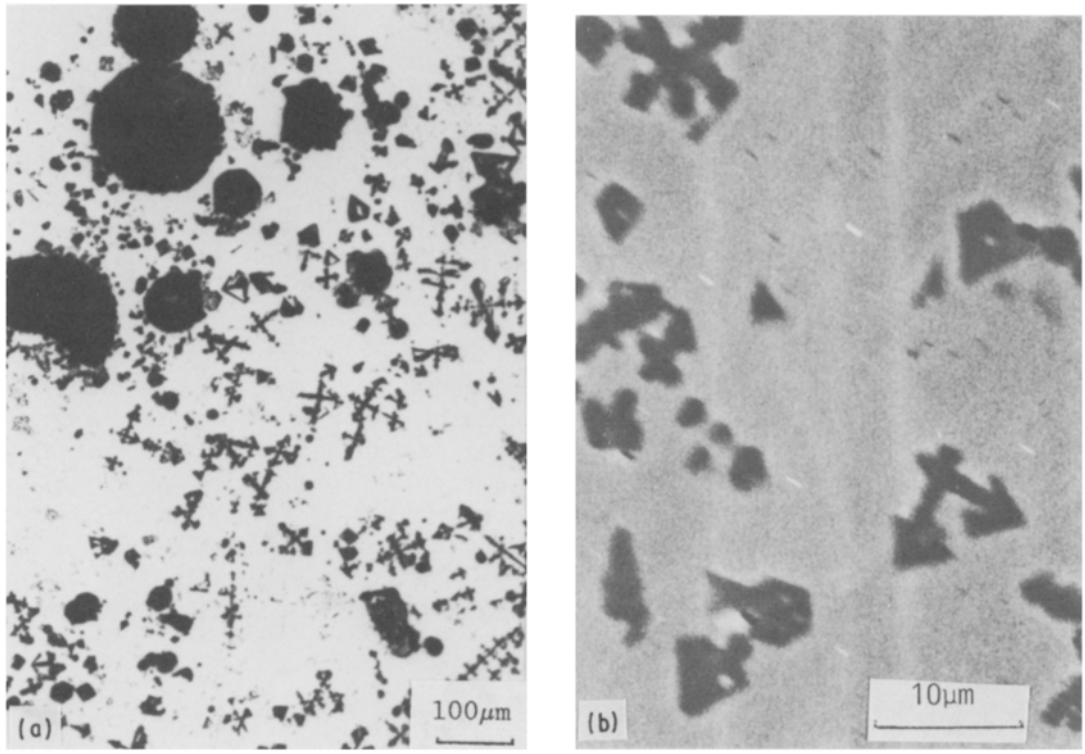

Figure 8 (a) Typical optical and (b) SEM photomicrographs of reacted TiNi product. The black phase is Ti_2Ni, except for the larger black areas in (a) which are porosity.

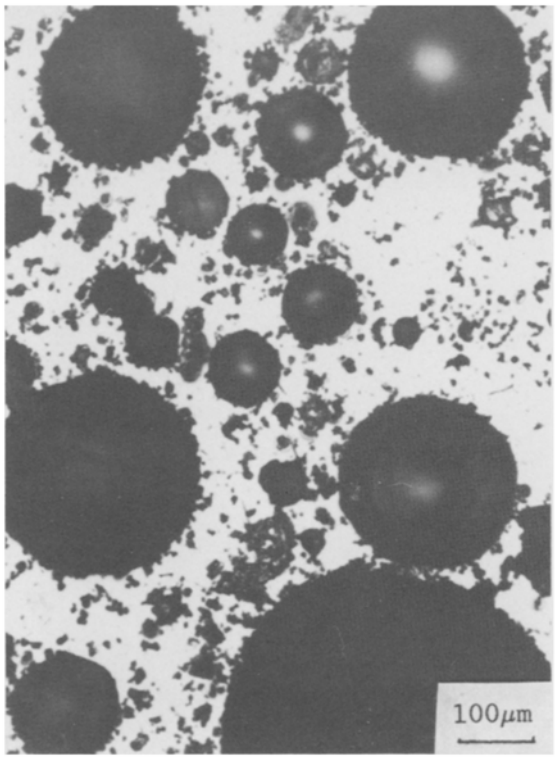

Figure 9 Optical photomicrograph of the dilution-reacted sample (30% dilution) with a high degree of porosity.

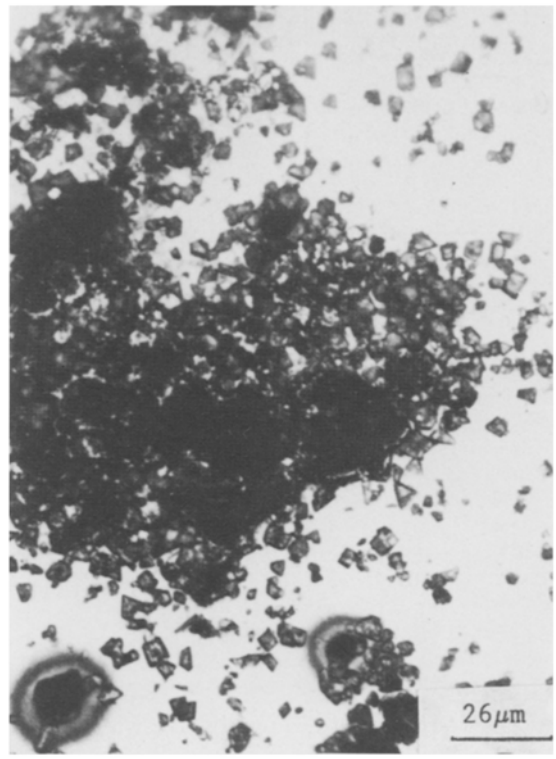

Figure 10 Optical photomicrograph showing Ti_2Ni segregation in a 30% dilution-reacted sample.

temperature increased considerably as the heating rate increased, showing the heat generated by the exothermic reaction increased with increase in heating rate. Increased heat generation can also result in an increase in the density of the product, whereas increasing the nickel particle size usually decreases the heat generated by the reaction.

The present investigation has not shown these trends in that both the heating rate and particle size did not greatly affect the combustion reaction. For instance, increasing the heating rate from 15 K min^{-1} to 1000 K min^{-1} increased the combustion temperature by only 100 K, whereas the ignition temperature decreased 25 K.

The increase in T_{ig} at lower heating rates was believed to be due to the formation of TiO_2 because titanium is very easily oxidized and the argon used was not sufficiently pure, i.e. up to 100 p.p.m. O_2 [15].

Considering the effect of dilution on the combustion process (Fig. 7) Equation 4 can be corrected to

$$(1 - v)(-\Delta H_f^0(T_{ig})) = \int_{T_{ig(v)}}^{T_m} C_{p_s}(p)\,dT + \Delta H_m + \int_{T_m}^{T_{c(v)}} C_{p_l}(p)\,dT \quad (6)$$

where v is the extent of dilution used, i.e. the fraction of the reactants which comprise the previously reacted TiNi.

Differentiating both sides with respect to v, and recording that $dT_{ig}(v)/dv = 0$ (Fig. 7), Equation 6 becomes

$$\Delta H_f^0(T_{ig}) = C_{p_l}(T_c)\frac{dT_c}{dv} \quad (7)$$

From Fig. 7, $dT_c/dv = -917.46$ K and $\Delta H_f^0(T_{ig})$ can be calculated from Equation 5. Therefore, from Equation 7

$$C_{p_l}(T_c) = 17.96\,\text{cal mol}^{-1}\,\text{K}^{-1}$$

Although T_c decreases on increasing dilution with TiNi, the heat capacity is still a constant value due to the fact that, in each case, the combustion products were in the liquid state (Fig. 7). The C_{p_l} value determined here is slightly larger than that predicted by an ideal solution of liquid nickel and titanium, i.e. 17.88 cal mol^{-1} K^{-1}.

Substituting the C_{p_l} value into Equation 1, it is possible to determine the heat of fusion of the TiNi intermetallic product: i.e. $\Delta H_m = 7.77 \pm 1.5$ kcal mol^{-1}. Based on this calculation it is possible to extend the enthalpy–temperature curve (Fig. 3) to include values for temperatures greater than the melting point of TiNi.

The accuracy of the above estimation depends on the accuracy of obtaining the experimental data, i.e. T_c, T_{ig} and dT_c/dv. From the present study it was sometimes noticed that the results were not always repeatable owing to the interactions between the liquid product and the thermocouple. Therefore, special precautions must be taken in order to obtain accurate data. Considering the inaccuracy of the experimental data and the slight change in ignition temperature (Fig. 6), it is suggested that the error associated with this determination of ΔH_m of TiNi was ± 1.5 kcal mol^{-1}.

6. Conclusions

Solidified TiNi intermetallic compounds have been synthesized using the thermal explosion mode of the SHS method in an argon atmosphere. The

combustion temperatures depended on heating rate and degree of dilution, whereas ignition temperature remained unchanged with respect to these processing parameters. Using the thermal explosion mode of combustion synthesis, the heat capacity for liquid-phase TiNi intermetallic ($C_{p_l} = 17.96\,\text{cal}\,\text{mol}^{-1}\,\text{K}^{-1}$) and the heat of fusion of the TiNi intermetallic product ($\Delta H_m = 7.77 \pm 1.5\,\text{kcal}\,\text{mol}^{-1}$) have been determined. These thermodynamic functions for TiNi are not available from the existing literature.

References

1. Z. A. MUNIR, *Ceram. Bull.* **67** (1988) 342.
2. H. C. YI and J. J. MOORE, *J. Mater. Sci.* **24** (1989) 3456.
3. A. G. MERZHANOV and F. F. BOROVIUSKAYA, *Comb. Sci. Tech.* **10** (1975) 195.
4. L. M. SHEPPARD, *Adv. Mater. Processes* February (1986) 25.
5. Y. S. NAIBORODENKO, V. I. ITIN and K. V. SAVITSKII, *Sov. Powd. Metall. Met. Ceram.* 7 (91) (1970) 562.
6. A. P. HARDT and P. V. PHUNG, *Comb. Flame* **21** (1973) 77.
7. A. P. HARDT and R. W. HOLSINGER, *ibid.* **21** (1973) 91.
8. H. MARGOLIN, E. ENCE and J. P. NIELSEN, *Trans. AIME* **197** (1953) 243.
9. C. M. WAYMAN and K. SHIMIZU, *J. Mater. Sci.* **6** (1972) 175.
10. V. I. ITIN, Y. S. NAIBORODENKO, A. D. BRATCHIKOV, N. P. BUTKEVICH, S. V. KOROSTELEV and L. V. SHOLOKHOVA, *Sov. Phys. J.* **18** (1976) 408.
11. A. D. BRATCHIKOV, A. G. MERZHANOV, V. I. ITIN, V. N. KHACHIN, E. F. DUDAREV, V. E. GYUNTER, V. M. MASLOV and D. B. CHERNOV, *Sov. Powd. Metal. Met. Ceram.* **19** (205) (1980) 5.
12. I. BARIN, O. KNACKE and O. KUBASCHEWDKI, "Thermochemical Properties of Inorganic Substances", Suppl. (Springer Verlag, 1977).
13. V. I. ITIN, A. D. BRATCHIKOV, V. N. DORONIN and G. A. PRIBYTKOV, *Sov. Phys. J.* **24** (1981) p. 1134.
14. V. I. ITIN, A. D. BRATCHIKOV, A. G. MERZHANOV and V. M. MASLOV, *Comb. Explos. Shock Waves* **17** (1981) 293.
15. H. C. YI and J. J. MOORE, *J. Mater. Sci.* **24** (1989) in press.
16. V. M. MASLOV, I. P. BOROVINSKAYA and A. G. MERZHANOV, *Comb. Explos. Shock Wave* **12** (1976) 631.
17. K. A. PHILPOT, Z. A. MUNIR and J. B. HOLT, *J. Mater. Sci.* **22** (1987) 159.

Received 18 July
and accepted 21 November 1988